30-band k.p method for quantum semiconductor heterostructures

Soline Richard, Faycal Raouafi, Alexandre Bondi, Laurent Pedesseau, Claudine Katan, Jean-Marc Jancu, Jacky Even

30-band k·p method for quantum semiconductor heterostructures

S. Boyer-Richard,[1] F. Raouafi,[2] A. Bondi,[1] L. Pédesseau,[1] C. Katan,[1] J.-M. Jancu,[1] and J. Even[1,a)]
[1]*Université Européenne de Bretagne, INSA, FOTON, UMR 6082, 35708 Rennes, France*
[2]*Laboratoire de Physico-chimie des Matériaux Polymères, Institut Préparatoire aux Etudes Scientifiques et Techniques, BP51, 2070 La Marsa, Tunisia*

(Received 28 December 2010; accepted 19 May 2011; published online 23 June 2011)

We illustrate how the linear combination of zone center bulk bands combined with the full-zone **k·p** method can be used to accurately compute the electronic states in semiconductor nanostructures. To this end we consider a recently developed 30-band model which carefully reproduces atomistic calculations and experimental results of bulk semiconductors. The present approach is particularly suited both for short-period superlattices and large nanostructures where a three-dimensional electronic structure is required. This is illustrated by investigating ultrathin GaAs/AlAs superlattices. © *2011 American Institute of Physics*. [doi:10.1063/1.3600643]

As high-performance computers are becoming more affordable, atomic-scale modeling is gaining importance as an investigative tool in materials science. Complementary *ab initio* and empirical approaches within atomic-scale simulations provide detailed information about the physical properties of materials. While first principles techniques, such as density functional theory, are well suited to predict structural and electronic properties over a large energetic region, the calculation of the excited-state manifold of semiconductors is still unsatisfactory.[1] In addition, they remain limited to small supercells because of computational cost. The empirical pseudopotential method (EPM) was successfully employed to describe the electronic properties of long period semiconductor superlattices[2] (SLs). This work was later extended to strained nanostructures using the linear combination of bulk bands (LCBB) (Ref. 3) approach. LCBB has demonstrated to be efficient in the calculation of the electron and hole single particle eigenstates of semiconductor quantum dots.[4] Indeed, full zone Bloch functions form a complete orthonormal set of functions (COSFs). A precise band-structure description can also be obtained for heterostructures, with a unique submillielectron volt precision throughout the Brillouin zone (BZ), using a spds* nearest-neighbor tight-binding (TB) model including spin–orbit coupling.[5–8] In that case accurate parameters have been optimized for bulk materials to achieve improved agreement with experiment.[9]

On the other hand, the need for simple and nonatomistic methods has led to the development of the **k·p** method and the envelope function approximation (EFA).[10] The **k·p**/EFA is often used to accurately interpret the excited-state properties of semiconductor SLs and nanostructures but it suffers from several drawbacks such as the description of interface band mixing that exists even for media with no difference in Bloch functions.[11] In the EFA, the nanostructure electronic wave functions are in fact implicitly developed on linear combination of Luttinger–Kohn (LCLK) functions which also form a COSF.[12] While a meaningful description of the optical properties of many bulk semiconductors can be obtained within the eight-band Kane model near the BZ center,[3] at least 30 bands are required for **X** and **L** points.[4] An improved derivation of the **k·p**/EFA was proposed later,[13] using explicit expansions o the heterostructure wave functions on LCLK. This complex **k·p**/LCLK theory has been rarely used, except to propose a new ordering of differential operators in the **k·p**/EFA.[14] A second example is the pseudopotential-derived multiband **k·p** method, without spin–orbit coupling, which was proposed for large systems (>10 000 atoms) and tested on GaAs/AlAs SLs by Wang and Zunger.[15] They demonstrated that LCBB and the LCLK are equivalent, provided that unitary transformations exist between the zone center bulk states of various semiconductors forming the heterostructure. It was also shown that a minimum set of 15 basis functions are required to obtain a correct description of the electronic states of bulk materials and the GaAs/AlAs SLs along the Γ-**X** line.

In this letter, we propose an alternative to the pseudopotential-derived multiband **k·p**/LCLK approach[15] by starting from a fully empirical 30-band **k·p** bulk model.[16–18] This allows an empirical modeling of bulk experimental band parameters and simple inclusion of spin–orbit coupling. First, we present our 30-band **k·p** model for bulk semiconductors and the **k·p**/LCLK method. As an illustration, we perform band-structure calculations of ultrashort period AlAs/GaAs [001] SLs.

The **k·p** method is usually used as a perturbation method to describe the band structure near a given **k** point of the BZ. It may also work over the full BZ if a large basis set of Bloch states is taken into account, as demonstrated in the

TABLE I. Dipole matrix elements of AlAs in definition of Ref. 16. Energies $E_{Pj}^{(\prime)}$ and matrix elements $P_{Pj}^{(\prime)}$ are linked by $E_{Pj}^{(\prime)}=2m_0/\hbar^2[P_j^{(\prime)}]^2$.

AlAs	E_P	E_{PX}	E_{Pd}	E_{PXd}	E_{p3}	E_{P3d}	E_{P2}	E_{P2d}	E_{PS}	E_{PU}	E'_P
eV	19.14	14.29	0.01	8.49	3.99	9.29	0.032	15.01	1.79	16.00	0.140

a)Author to whom correspondence should be addressed. Electronic mail: jacky.even@insa-rennes.fr.

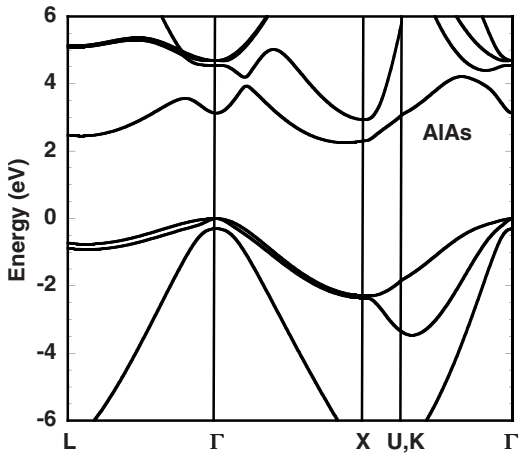

FIG. 1. Electronic band structure of bulk AlAs calculated with the 30-band $\mathbf{k}\cdot\mathbf{p}$ model at T=0 K. The model parameters are given in Table I and some values of the band energies and effective masses in Table II.

seminal work of Cardona and Pollak.[18] They used a 15 $\times$15 $\mathbf{k}\cdot\mathbf{p}$ Hamiltonian without the spin–orbit interaction and obtained a correct description of the valleys of the lowest lying conduction band and valence bands in bulk Si and Ge. However, many new generation device concepts rely on the spin-related properties of semiconductor nanostructures[19] so that relativist corrections to the band structure have to be considered. The 30-band $\mathbf{k}\cdot\mathbf{p}$ method is an extension of Cardona and Pollak's work with the inclusion of the spin–orbit interaction and a direct fit of the Hamiltonian matrix elements from the experimental band parameters. The quantities included in the fitting procedure are the effective masses and the valence and conduction band energies at Γ, **X**, and **L**. It was shown to be valid for Si and Ge in describing the bulk energy states up to 5 eV above the valence band maximum on the first BZ.[16] This leads to an accuracy comparable to calculations with the spds* TB models.[9] For diamondlike crystals, the 30$\times$30 $\mathbf{k}\cdot\mathbf{p}$ Hamiltonian is completely determined by ten independent parameters and this number grows to eighteen for zinc-blende compounds because of the lack of inversion symmetry. The model parameters can be reduced to eleven for III–V semiconductors without worsening the fit of band structures.[16] The parameter values for AlAs are given in Table I and their definitions can be found in Ref. 16. Figure 1 shows the corresponding band structure. Results are found to be in good agreement with the TB calculations all around the BZ and the calculated conduction band minimum (CBM) agrees with the experimental value.[20] In addition, the reduced masses and Luttinger parameters compare well with the experimental[20] and TB results as seen in Table II. The crucial point of the 30$\times$30 $\mathbf{k}\cdot\mathbf{p}$ method is the continuity between U [1,1/4,1/4] and K [0,3/4,3/4], equivalent points of the BZ which is not obtained by construction in contrast with atomistic approaches as pseudopotential or TB schemes. This discrepancy, observed in an earlier 30-band $\mathbf{k}\cdot\mathbf{p}$ parametrization of AlAs (Ref. 21) is corrected in the present work except for the second conduction band which is inherent to the formalism.[18]

The $\mathbf{k}\cdot\mathbf{p}$ method in EFA is widely used to find the band structure and wave functions of heterostructures.[10,22] The basic assumption in the EFA approach is the similarity between the matrix elements in the Hamiltonian for most of the semiconductor compounds near the zone center. Only zone center Bloch functions $u_{n,\vec{k}=0}(\vec{r})$ are used in the expansion of the heterostructure wave functions (n=1–8 in the eight-band $\mathbf{k}\cdot\mathbf{p}$ method). In the EFA, the $u_{n,0}(\vec{r})$ are considered equal in all the materials and it is not necessary to give an explicit expression for them. When considering folded **X** states in a [001] quantum heterostructure, all these approximations appear to be severe shortcomings.[15]

In this work, we used a fully empirical 30-band $\mathbf{k}\cdot\mathbf{p}$ bulk model instead of the pseudopotential-derived multiband $\mathbf{k}\cdot\mathbf{p}$ Hamiltonian.[15] It allows an empirical modeling of bulk experimental band parameters but also the inclusion of spin–orbit coupling in a simple way. Moreover, a new block-diagonalization of the 30$\times$30 $\mathbf{k}\cdot\mathbf{p}$ Hamiltonian into two equivalent 15$\times$15 blocks was introduced to calculate the dispersions of the bulk electronic states along the Γ-**X** line. Our $\mathbf{k}\cdot\mathbf{p}$/LCLK approach is then based on linear combinations of only 15 LK functions $\varphi_{n,\vec{k}}(\vec{r})=u_{n,0}(\vec{r})e^{i\vec{k}.\vec{r}}$, the reduced 15$\times$15 blocks of the 30-band $\mathbf{k}\cdot\mathbf{p}$ Hamiltonian being used to find the matrix elements. Contrary to the pseudopotential-derived multiband $\mathbf{k}\cdot\mathbf{p}$ model,[15] LK functions must be obtained independently. In order to keep the model as simple as possible, a basic EPM (Ref. 23) without spin–orbit coupling has been used to obtain zone center Bloch functions in each material (GaAs and AlAs). These functions were developed on 15 symmetrized combinations of plane waves.[24] It preserves unitary transforms between the 15 basis functions of the various bulk materials.[15] Clebsch–Gordan coefficients were finally used to yield symmetry-adapted functions fully compatible with the basis of the 30-band $\mathbf{k}\cdot\mathbf{p}$ bulk model.[16] In other words, a precise determination of the eigenenergies is combined with simple but symmetry-adapted expressions of bulk eigenstates wave functions. We may notice that this is the only point at which atomistic information is directly introduced into the calculations. The nanostructure wave functions are expanded on the LK functions of a given material in the heterostructure (e.g., A and B, respectively, for GaAs and AlAs in a GaAs/AlAs SL):$\Psi_{NS}(\vec{r})=\Sigma_{n,\vec{k}}c_{n,\vec{k}}\varphi^{A}_{n,\vec{k}}(\vec{r})$. Structure factors are introduced

TABLE II. Comparison of the Luttinger parameters, effective masses, and energy levels, obtained in the present work with the 30-band $\mathbf{k}\cdot\mathbf{p}$ model and compared to the spds* TB calculations and experimental values (Ref. 16).

	γ_1	γ_2	γ_3	$m(\Gamma)$	$m_t(X)$	$m_l(X)$	$m_t(L)$	$m_l(L)$	X_{6c}	X_{7v}	L_{6c}
GaAs ($\mathbf{k}.\mathbf{p}$)	7.18	2.23	2.99	0.067	0.23	1.16	0.11	1.67	1.94	−2.62	1.75
GaAs (TB)	7.51	2.18	3.16	0.067	0.23	1.24	0.12	1.53	1.99	−3.05	1.85
GaAs (exp)	6.85	2.1	2.9	0.067	0.23	1.3	0.08	1.9	1.98	−2.80	1.85
AlAs ($\mathbf{k}\cdot\mathbf{p}$)	3.76	0.82	1.42	0.15	0.22	0.97	0.15	1.32	2.26	−2.29	2.48
AlAs (TB)	3.85	0.69	1.47	0.156	0.23	1.4	0.16	1.37	2.19	−2.51	2.67
AlAs (exp)	3.69	0.79	1.40	0.146	0.226	1.27	0.14	1.09	2.22	−2.41	2.54

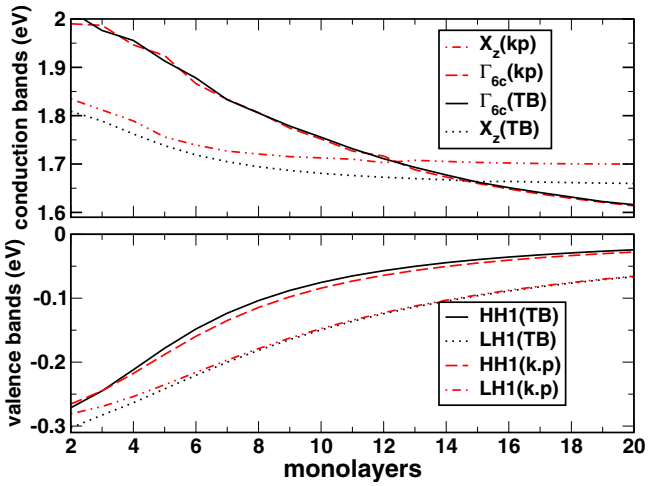

FIG. 2. (Color online) Comparison of the near-band gap energies of the $(GaAs)_n/(AlAs)_n$ SL at the zone center of the BZ as function of period **n**. Full and dot lines correspond to TB results, while dash and dash-dot lines correspond to $\mathbf{k}\cdot\mathbf{p}$ results. The energy zero is taken at the bulk GaAs valence band maximum.

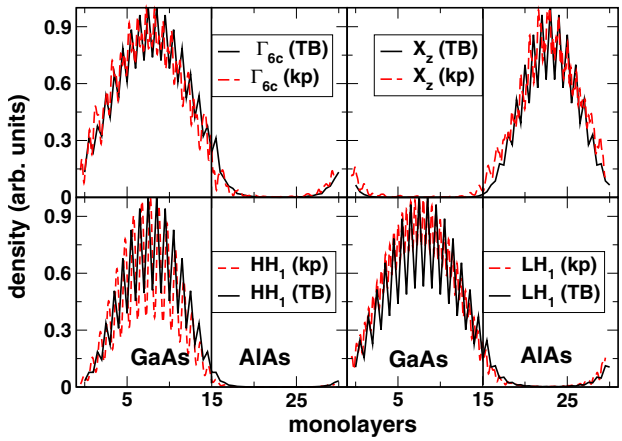

FIG. 3. (Color online) Hole and electron wave functions of the $(GaAs)_{15}/(AlAs)_{15}$ SL obtained with the 30-band $\mathbf{k}\cdot\mathbf{p}$ (dash lines) and TB (full lines) models.

to take into account unitary transforms between the Bloch functions of bulk materials.[15] The resulting $\mathbf{k}\cdot\mathbf{p}$/LCLK approach is an improvement over the conventional $\mathbf{k}\cdot\mathbf{p}$ method in EFA with low computational cost as compared to atomistic methods like the EPM associated to LCBB or[3,4] extended-basis spds* TB schemes.[5–9]

We illustrate application of our $\mathbf{k}\cdot\mathbf{p}$/LCLK model by considering the case of $(GaAs)_\mathbf{n}/(AlAs)_\mathbf{n}$ SLs grown lattice-matched on a GaAs substrate. Such heterostructures provide a stringent test for evaluating the performance of *ab initio* and empirical approaches,[2,3,25] as the CBM occurs at a **k**-point different from Γ and depending on the SLs period **n**. In our calculations, the valence band offset has been chosen in accordance with experimental data: $\Delta E_v = 0.55$ eV.[20,26] Figure 2 compares the $\mathbf{k}\cdot\mathbf{p}$ and TB near-band-gap energy levels at Γ of the $(GaAs)_\mathbf{n}/(AlAs)_\mathbf{n}$ SLs as a function of the number of monolayers (MLs) **n**.

The two models agree well for the valence and Γ-like conduction states owing to similarity of the band parameters (Table II). The Xz-levels stem from the bulk AlAs X_{6c}-states folded in the center of the SL BZ. Their variations with **n** slightly differ in the two calculations because of difference in energy position of bulk X6c-states (Table II). In the 30-band $\mathbf{k}\cdot\mathbf{p}$ model, the quantum size effect associated with the SL period induces a $Xz \rightarrow \Gamma_{6c}$ crossover for the critical thickness $\mathbf{n}=\mathbf{nc}\approx 13$ MLs. It agrees nicely with the experimental value at low temperature, $\mathbf{nc}\approx 14$,[2,3] and the present TB result. This corresponds to a significant improvement over pseudopotential-derived multiband $\mathbf{k}\cdot\mathbf{p}$ calculations[3] where **nc** is found at 7 MLs, as a result of GaAs conduction band mass overestimation. Interestingly, the resulting $\mathbf{k}\cdot\mathbf{p}$ gap energies become closer to the experimental data for all periods,[2] underlying the quality of the present $\mathbf{k}\cdot\mathbf{p}$/LCLK approach. For $\mathbf{n}>\mathbf{nc}$ the CBM is a Γ-like state localized in the GaAs well as evidenced in Fig. 3 for the $(GaAs)_{15}/(AlAs)_{15}$ SL. Again, we obtain a good agreement between the TB and $\mathbf{k}\cdot\mathbf{p}$ results for the electron and hole wave functions.

In this work we have proposed a 30-band $\mathbf{k}\cdot\mathbf{p}$/LCLK model that allows for simple description of the band diagram of zinc-blende semiconductors or quantum nanostructures in the whole BZ. It relies on very few adjustable parameters. This is illustrated by modeling the electronic states of the AlAs/GaAs benchmark SLs. Results show a nice agreement with both atomistic calculations and experimental data. Contrarily to standard $\mathbf{k}\cdot\mathbf{p}$/EFA schemes, BZ folding effects are well accounted for. In fact, the $Xz \rightarrow \Gamma_{6c}$ crossover is correctly predicted for short-period $(GaAs)_\mathbf{n}/(AlAs)_\mathbf{n}$ SLs.

This work was granted access to the HPC resources of CINES under the allocation 2010-[c2010096472] made by GENCI (Grand Equipement National de Calcul Intensif).

[1]P. Rinke, A. Qteish, J. Neugebauer, C. Freysoldt, and M. Scheffler, New J. Phys. **7**, 126 (2005), and references therein.
[2]D. M. Wood and A. Zunger, Phys. Rev. B **53**, 7949 (1996).
[3]L. W. Wang and A. Zunger, Phys. Rev. B **59**, 15806 (1999).
[4]G. Bester, X. Wu, D. Vanderbilt, and A. Zunger, Phys. Rev. Lett. **96**, 187602 (2006).
[5]J.-M. Jancu, R. Scholz, G. C. La Rocca, E. A. de Andrada e Silva, and P. Voisin, Phys. Rev. B **70**, 121306 (2004).
[6]M. Virgilio and G. Grosso, Phys. Rev. B **79**, 165310 (2009).
[7]N. Kharche, S. Kim, T. B. Boykin, and G. Klimeck, Appl. Phys. Lett. **94**, 042101 (2009).
[8]F. Sacconi, A. Di Carlo, P. Luigli, M. Städele, and J.-M. Jancu, IEEE Trans. Electron Devices **51**, 741 (2004).
[9]J. M. Jancu, R. Scholz, F. Beltram, and F. Bassani, Phys. Rev. B **57**, 6493 (1998).
[10]G. Bastard and J. A. Brum, IEEE J. Quantum Electron. **22**, 1625 (1986).
[11]B. A. Foreman, Phys. Rev. Lett. **81**, 425 (1998).
[12]J. M. Luttinger and W. Kohn, Phys. Rev. **97**, 869 (1955).
[13]M. G. Burt, J. Phys.: Condens. Matter **4**, 6651 (1992).
[14]B. A. Foreman, Phys. Rev. B **48**, 4964 (1993).
[15]L. W. Wang and A. Zunger, Phys. Rev. B **54**, 11417 (1996).
[16]S. Richard, F. Aniel, and G. Fishman, Phys. Rev. B **70**, 235204 (2004).
[17]C. R. Pidgeon and R. N. Brown, Phys. Rev. **146**, 575 (1966).
[18]M. Cardona and F. Pollak, Phys. Rev. **142**, 530 (1966).
[19]I. Žutić, J. Fabian, and S. Das Sarma, Rev. Mod. Phys. **76**, 323 (2004).
[20]*Semiconductors: Intrinsic Properties of Group IV Elements and III-V, II-VI and I-VII Compounds*, Landolt-Börnstein, New Series, Group III Vol. 22, Pt. A, edited by O. Madelung (Springer, Berlin, 1987).
[21]N. Fraj, I. Saïdi, S. Ben Radhia, and K. Boujdaria, J. Appl. Phys. **102**, 053703 (2007).
[22]J. Even, F. Dore, C. Cornet, and L. Pedesseau, Phys. Rev. B **77**, 085305 (2008).
[23]J. R. Chelikowsky and M. L. Cohen, Phys. Rev. B **14**, 556 (1976).
[24]F. Bassani and M. Yoshimine, Phys. Rev. **130**, 20 (1963).
[25]R. Scholz, J.-M. Jancu, F. Beltram, and F. Bassani, Phys. Status Solidi B **217**, 449 (2000).
[26]I. Vurgaftman and J. R. Meyer, J. Appl. Phys. **94**, 3675 (2003).